Int. J. Electrochem. Sci., 6 **(2011)** 4239 - 4249

International Journal of
ELECTROCHEMICAL
SCIENCE
www.electrochemsci.org

Synthesis and Characterization of Lithium Trivanadates as Cathode Materials for Rechargeable Lithium Battery via a New Wet Chemical Synthesis Method

Xiao-Yu Cao[1,2,*], *Li-Xu Zhang*[1,2], *Bin Yang*[3], *Xing Liu*[1,2], *Da-Wei Song*[1,2], *Ling-Bo Qu*[1,2]

[1] School of Chemistry and Chemical Engineering, Henan University of Technology, Zhengzhou 450001, People's Republic of China
[2] Zhengzhou (China-Italy Cooperation) Key Laboratory of Clean Energy, Henan University of Technology, Zhengzhou 450001, People's Republic of China
[3] Zhengzhou Sci-Tech and Information Institute, Zhengzhou 450007, People's Republic of China
[*]E-mail: caoxy@haut.edu.cn

Received: 20 July 2011 / *Accepted:* 2 August 2011 / *Published:* 1 September 2011

LiV_3O_8 powders were prepared via a facile wet chemical synthesis method starting from the stoichiometric $LiNO_3$ and LiCl as binary Li-source, and NH_4VO_3 as V-source. The as-prepared brownish red products were characterized by X-ray diffraction (XRD), scanning electron microscope (SEM), galvanostatic discharge/charge test, cycle voltammetry (CV) and electrochemical impedance spectroscopy (EIS). The results indicate that heating temperature has great influences on the crystallinity, morphology, particle size, and electrochemical performance of the thus-synthesized samples. As a result, the LiV_3O_8 obtained at 350 °C for 10 h displays excellent electrochemical properties because of its desirable crystallinity and preferred particle size. It is found that 350 ^oC–synthesized sample delivers the initial discharge capacity of 313.5 mAh g^{-1} in the range of 1.8–4.0 V at a current rate of 30 mA g^{-1} and remains 218 mAh g^{-1} after 40 cycles. CV result also shows that 350 ^oC–synthesized sample displays the good electrochemical reversibility. EIS fitting calculation implies that an active process may occur after a few cycles.

Keywords: LiV_3O_8, binary Li-source, cathode material, lithium-ion battery, electrochemical performances

1. INTRODUCTION

Since the lithium-ion battery has been commercialized, it has far-ranging application in electronic products. Only continuously improve the specific capacity of lithium ion battery can we

satisfy the needs of high energy application. It is well-known that the performance and cost of the lithium-ion battery mainly depend on the properties of cathode materials. Because the valence of vanadium element has a wide range, the lithium vanadium oxide $Li_{1+x}V_3O_8$ ($0 \le x \le 0.2$) shows high discharge capacity and energy density as cathode material for lithium-ion battery. Due to its low cost, facile preparation, and nice electrochemical performance, the $Li_{1+x}V_3O_8$ as a promising cathode material has become the hot research topic.

Dozens of studies indicate that the electrochemical performance of $Li_{1+x}V_3O_8$ is greatly influenced by the synthetic methods. In the early days, high-temperature melting is simply operated, however, not only it needs high temperature, but also the product often has low specific capacity and poor cycling performance [1]. Aiming at overcoming the shortcomings of high-temperature melting, some soft chemistry synthesis methods (SCSMs) have been proposed, such as hydrothermal treatment [2–4], rheological phase reaction [5,6], combustion synthesis method [7], quick quenching [8], sol-gel method [9–13]. These methods can be mainly grouped into the two aspects to optimize the electrochemical properties of $Li_{1+x}V_3O_8$ products. One is modifying the raw materials or adding structure-modifying agents that make the reaction more entirely. Especially when vanadium oxides are used as V-source, the freshly home-prepared vanadium oxides are more active than the commercial ones. For example, J.G. Xie et al. [10] synthesized high capacity $Li_{1.2}V_3O_8$ from V_2O_5 gel prepared by polycondendation of vanadic acid, and H.M. Liu et al. [14] obtained single-crystalline LiV_3O_8 using VO_2 nanorods made from the commercial V_2O_5 and n-butanol by a hydrothermal method. Adding structure-modifying agent is an effective method to improve the performance of LiV_3O_8, for instance, the addition of citric acid [5], tartaric acid [12], EDTA [13], oxalic acid [15], and PEG [15,16] makes the reaction reach the best possible homogeneity. Another way is altering the calcining condition or post-treatment manner. For example, F. Wu et al. [17] obtained LiV_3O_8 by sintering the precursor in microwave furnace at 450 ^oC for 80 mins. Y.M. Liu et al. [18] synthesized pure-phase $Li_{1.2}V_3O_8$ by ultrasonically treatment for 90 mins. And H.M. Liu et al [11] obtained LiV_3O_8 with the optimal performance by a post-treating in argon atmosphere at 300 ^oC. By using kinds of these methods, the morphology, crystallinity, interlamellar spacing, and particle size of $Li_{1+x}V_3O_8$ products become more suitable for the diffusion of lithium ion and electrochemical intercalation/deintercalation reaction. Due to these advantages, the target products deliver superior electrochemical performance over the high-temperature melting products. But meanwhile, it cannot be ignored that the many SCSMs are very tedious and expanding the scope of application is not easy when referring to the excellent electrochemical performance of the SCSMs-derived $Li_{1+x}V_3O_8$ products.

In the investigation, we obtain LiV_3O_8 (x=0) via using stoichiometric $LiNO_3$ and LiCl as Li-source and NH_4VO_3 as V-source by a simple wet chemical method, then heat-treated at different temperatures. Afterward, we study the structure, morphology and electrochemical properties of the products, and find that they display the nice electrochemical performances.

2. EXPERIMENTAL

The LiV_3O_8 precursor was prepared by using $LiNO_3$ and LiCl as binary Li-source, NH_4VO_3 as V-source via the wet chemistry synthesis method. The typical preparation process is as follows. At first, $LiNO_3$, LiCl, and NH_4VO_3 at the stoichiometric ratio of 0.875:0.125:3 were dissolved in boiling re-distilled water in a beaker. After ultrasonically treated for 30 mins, the mixed solution was evaporated under magnetic stirring until the orange deposit was obtained. Second, the deposit was dried in the air atmosphere at 120 ^oC for overnight to get the LiV_3O_8 precursor. Subsequently, the precursor was calcined at 250 ^oC, 300 ^oC, and 350 ^oC for 10 hrs, respectively, in the muffle furnace. When it cooled to room temperature and then was grinded in the agate mortar, the brownish red LiV_3O_8 powders were obtained. The structural characterization of the as-prepared powders was conducted by a Rigaku D/Max-2500 powder diffractometer (Rigaku, Japan) with Cu Kα radiation (λ = 1.54056 Å). SEM investigation of the as-prepared powders was taken on a JSM-6510LV scanning electron microscope (JEOL, Japan). The cathode films were fabricated by incorporating the paste composed of the as-synthesized active powders, acetylene black (AB) and polytetrafluoethylene (PTFE) binder at a weight ratio of 80:10:10. The dried cutting disc films were loaded on the stainless-steel meshes to prepare the working electrodes. The CR2016 type coin cells were assembled using stainless-steel case purchasing from Shenzhen Meisen Machine-electro Equipment Co., Ltd, China in a high purified argon-filled dry box (JMS-3, Nanjing Jiumen Automation Technology Co., Ltd, China). The counter-electrode was lithium foils (Wuhan Newthree Technology Co., Ltd, China) and the separator was commercial polyethylene (PE) film (ND420 H129-100, Asahi Kasei Chemical Co., Japan). 1 mol dm^{-3} solution of $LiClO_4$ dissolving in the 1:1 mixture of ethylene carbonate and dimethyl carbonate (Zhangjiagang Guotai-Huarong New Chemical Materials Co., Ltd, China) was used as the electrolyte. The discharge/charge cycles were performed at the rate of 30 mA g^{-1} over a potential between 1.8 and 4.0 V at the room temperature on a multi-channel CT-3008W-5V5mA-S_4 battery tester (Shenzhen Neware Technology Co., Ltd, China). Cyclic voltammetry (CV) was carried out on a CHI660D electrochemical workstation (Chenhua, Shanghai) at a scan rate of 0.1 mV/s on the potential interval 1.8–4.0 V (vs. Li/Li^+) by using three electrodes system. EIS experiments were also performed at a CHI660D electrochemical workstation. The ac perturbation signal was ±5mV and the frequency range was from 10 mHz to 100 kHz.

3. RESULTS AND DISCUSSION

The XRD patterns of LiV_3O_8 powders calcined at different temperatures are shown in the Fig.1. The position and the intensity of the main diffraction peaks can be identified as LiV_3O_8 phase apart from a V_2O_5 impurity peak marked with the inverted triangle (▽), which is in conformity with that of standard data in the PDF no.13-248.

It is proved that at the very lower temperature, namely 250 ^{o}C, we can successfully achieve the LiV_3O_8 phase by the new synthesis process. However, over 600 ^{o}C is deemed necessary to prepare LiV_3O_8 through the conventional solid-state reaction.

With the increase of heating temperature, the relative intensity and the width of the (100) diffraction peak have some changes. It is found that the (100) diffraction peak becomes stronger and sharper with the temperature increasing. At the same time, it implies both the crystallinity and the particle size increase. It illustrates that the 300 ^{o}C–synthesized sample has the highest crystallinity and particle, which will be corroborated in the SEM result. Because the preferential orientation leads to a long path for the diffusion of Li^+ ion, high intensity of the (100) peak is disadvantage to Li^+ ion intercalation/deintercalation. Meanwhile, it means the poor electrochemical performance. So we can predict that the heating temperature is a significant influencing factor for the electrochemical performance of the thus-prepared products.

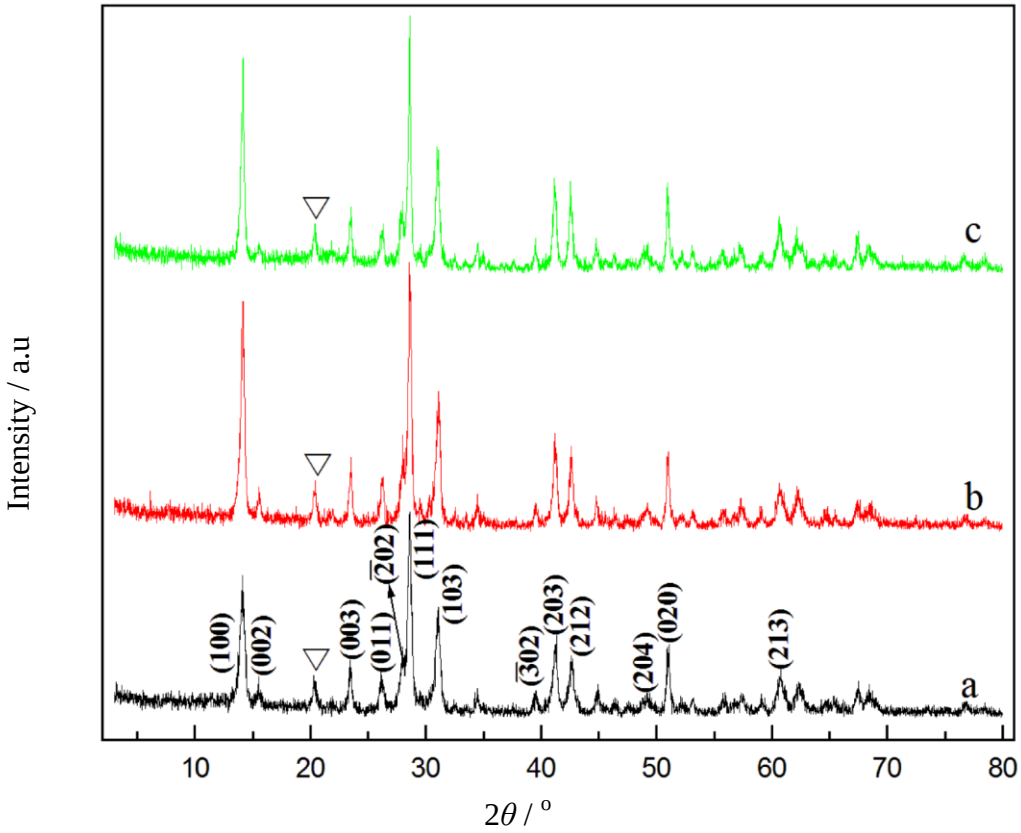

Figure 1. XRD patterns of LiV_3O_8 materials obtained at different temperatures (a) 250 °C, (b) 300 °C, (c) 350 °C.

The SEM images of LiV_3O_8 powders obtained by the new synthesis process at different heating temperatures are demonstrated in Fig. 2. As shown in Fig. 2(a-b), small lamellar crystallites together accummulate and form large-sized particles. And there are some fine needle-like crystallitues adhering to the outside of the lamellar crystallites for the 250 ^{o}C–synthesized sample. While with the heating

temperatures heighteninging, the obtained crystallities cummulate more compact, and the particle becomes larger. The 300 ^{o}C–synthesized sample appears the largest partical size, and its surfaces are somewhat coarser than the 350 ^{o}C–synthesized one. Many reserchers suggest that the morphology of the electrode material can make an important effect on its electrohemical performance [17–20]. If the active material has the larger particle size and anisotropic crystallinity, there will be a longer diffusion path for Li^{+} ions intercalation process, which is disadvantageous for improving the electrochmical perfrmace of sample. On the basis of the theory, we can surmmarize that the 300 ^{o}C–synthesized sample may has a poor electrochemical perfprmance.

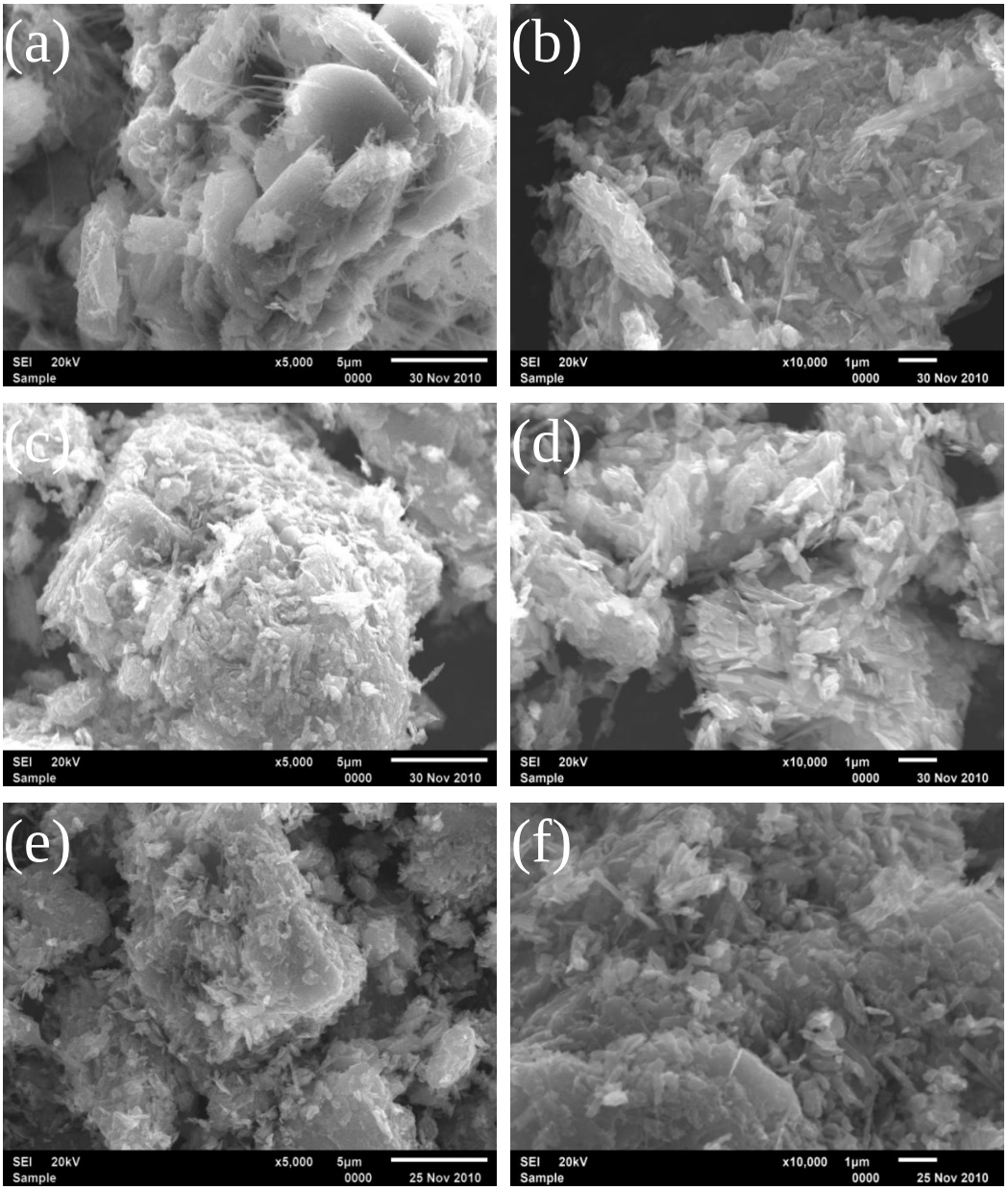

Figure 2. Different magnified SEM images of LiV_3O_8 podwer obtained at different heating tempertures (a-b) 250 ^{o}C, (c-d) 300 ^{o}C, (e-f) 350 ^{o}C

The initial discharge curves of the LiV_3O_8 obtained at different heating temperatures are shown in Fig.3. It is found that the first discharge specific capacities of LiV_3O_8 heated at 250 °C, 300 °C, and 350 °C are 311.15 mAh g^{-1}, 295.18 mAh g^{-1}, and 313.46 mAh g^{-1}, respectively. In addition, the shape of the three discharge curves is similar. From the open circuit voltage to about 2.8 V, the voltage drops sharply.

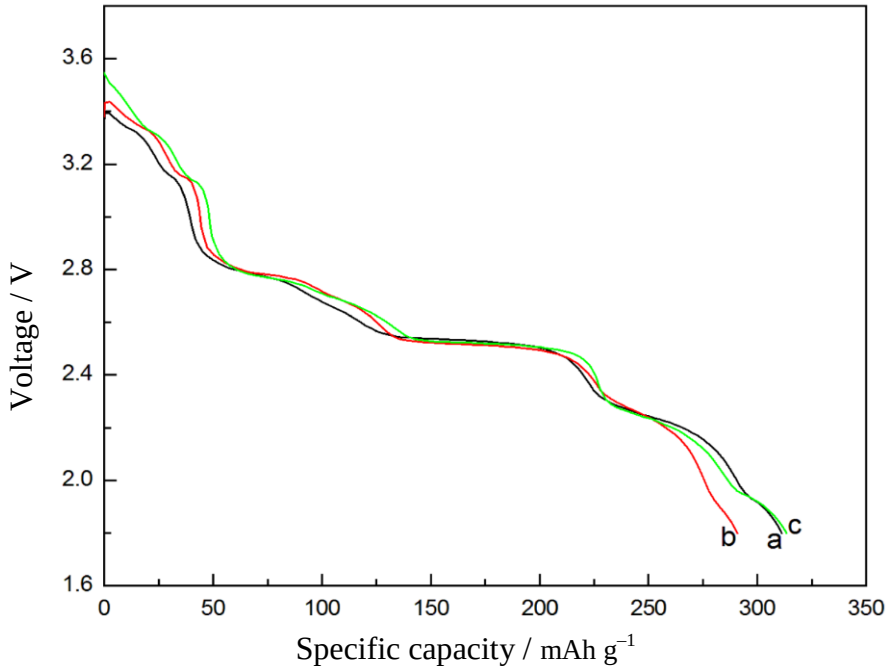

Figure 3. Initial discharge curves of LiV_3O_8 obtained at different heating temperatures (a) 250 °C, (b) 300 °C, (c) 350 °C.

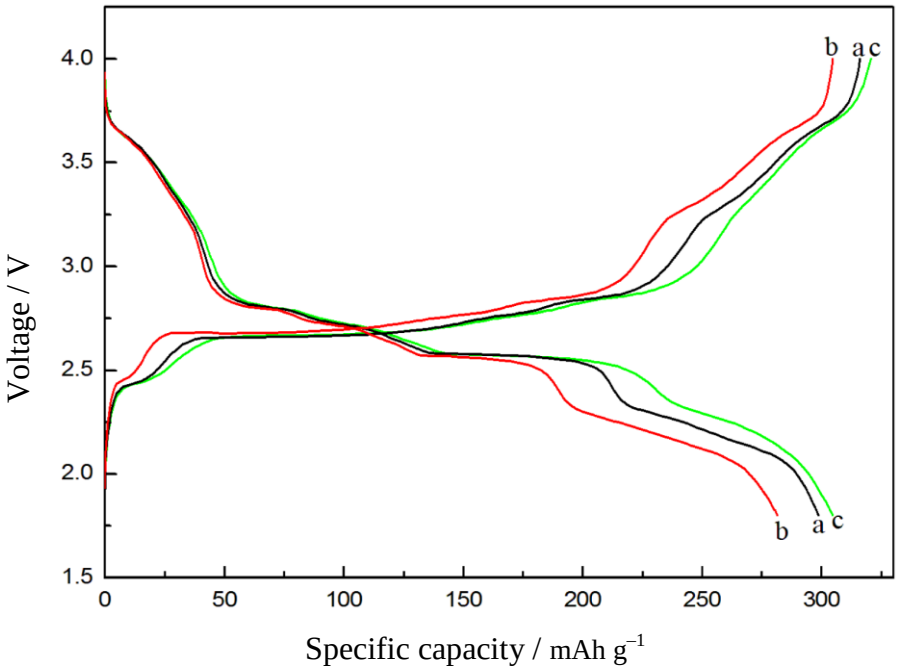

Figure 4. The third charge/discharge curves of LiV_3O_8 obtained at different heating temperatures (a) 250 °C, (b) 300 °C, (c) 350 °C.

The reason may be explained that the diffusion rate of Li^+ ion from electrolyte to electrode is slower than the electrochemical reaction rate at the interface of electrode/electrolyte at the beginning of electrochemical reaction. This phenomenon is defined as the electrode polarization. However, the voltage begins to drop slowly at the stage from 2.8 V to 2.5 V. Especially on the 2.5 V, the discharge curve almost is flat. This may be ascribed to a phase transition process, which determines the main discharge capacity for LiV_3O_8 materials. Below 2.5 V, voltage drops rapidly, which suggests that there is another polarization process putting off the electrode reaction. The charge/discharge curves at the 3rd cycle are illustrated in Fig.4. Whatever the discharge or charge specific capacity, the 350 ^oC–synthesized sample achieves the maximum capacity. In addition, it also displays the highest discharge plateau and the lowest charge plateau according to the curves. The length of second and third plateau is the crucial step dominating the specific capacity. We consider that the main reason for the different discharge/charge capacities of LiV_3O_8 samples may be associated with the crystallinity and morphology of the materials. In the case of LiV_3O_8 materials, the improvement of crystallinity makes electrode polarization become enlargement and phase transition become harder, which both decrease the specific capacity. On the other hand, the larger particle size also contributes to the lower capacity. Considering the higher crystallinity and larger particle size for sample obtained at 300 ^oC, it displays a lower capacity than the others.

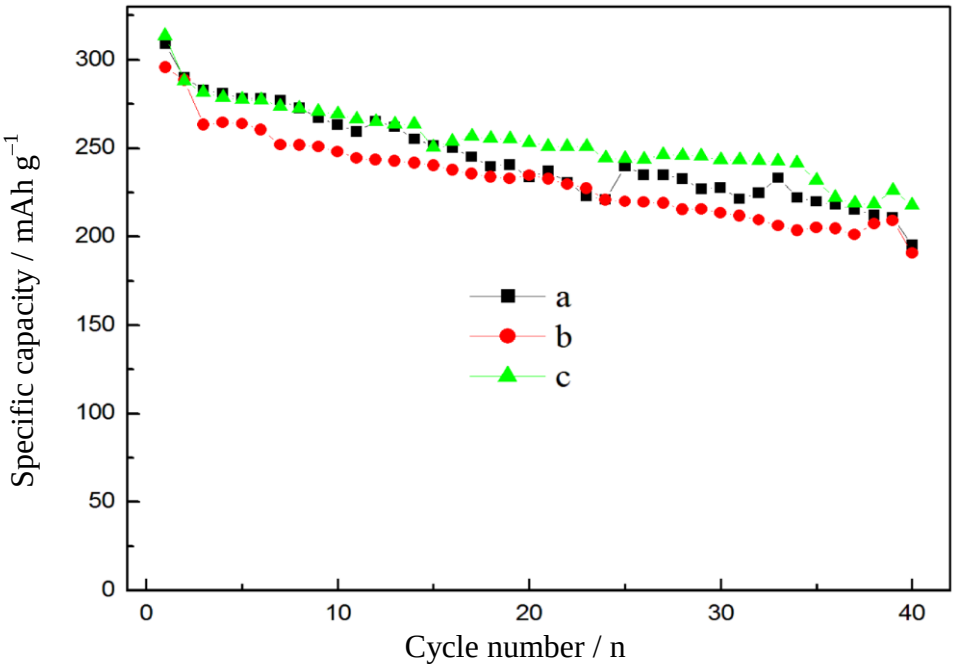

Figure 5. Cycling stability curves of LiV_3O_8 obtained at different heating temperatures (a) 250 ^oC, (b) 300 ^oC, (c) 350 ^oC.

The cyclical stability of LiV_3O_8 synthesized by the new synthesis route obtained at different heating temperatures is presented in Fig.5. It can be seen that the 350 ^oC–synthesized sample shows

the best cycleability. Its initial specific capacity is 313.5 mAh g^{-1}, and it remains 218 mAh g^{-1} after 40 cycles. When it comes to the products obtained at 250 ^{o}C and 350 ^{o}C for 10 hrs, they have the approximate capacity before the former 10 cycles. But after 10 cycles, the specific capacity of 250 ^{o}C–synthesized sample declines rapidly. The reason may be the presence of bound water molecules [1] which are not eliminated enough at 250 ^{o}C in the lattice of LiV_3O_8. And the presence of a bit amount of water is beneficial to the diffusion of Li^+ ion due to expanding the interlayer spacing. With the times of electrochemical reaction prolonging, water molecules losing from the interlayer spacing will lead to capacity fading. However, the 300 ^{o}C–synthesized LiV_3O_8 sample has the lowest initial specific capacity and the worst cycling stability. In terms of the XRD and SEM results, the phenomenon may be ascribed to its highest crystallinity and largest particle size. On the whole, the products prepared by the new method demonstrate a better cycling stability.

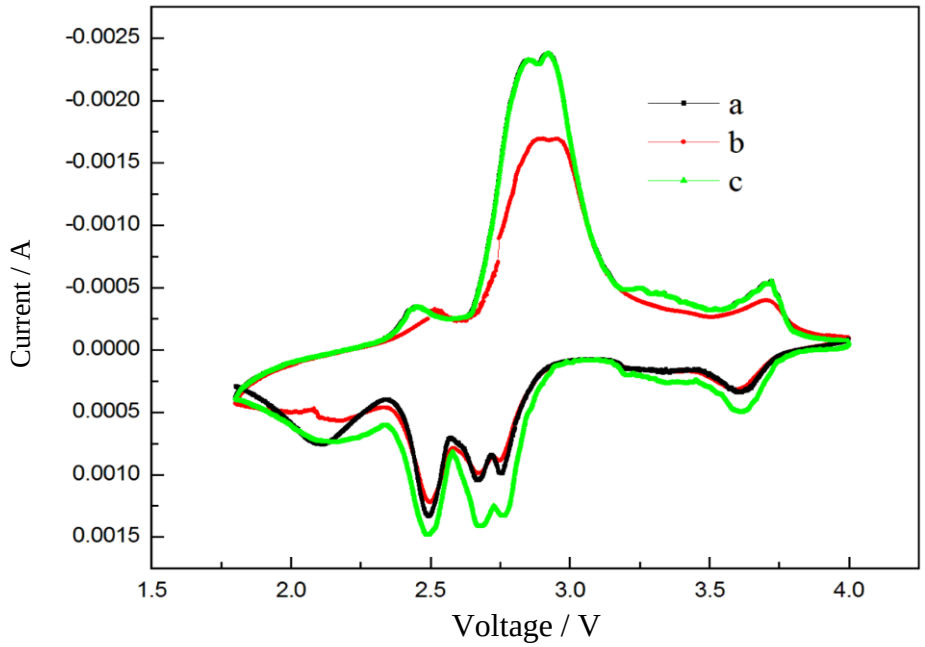

Figure 6. The fifth cyclic voltammograms of LiV_3O_8 obtained at different heating-treated temperatures (a) 250 ^{o}C, (b) 300 ^{o}C, (c) 350 ^{o}C.

The Fig.6 shows the comparisons of the fifth cyclic voltammograms for LiV_3O_8 samples heated at different temperatures. As seen in the curves of 350 ^{o}C–synthesized sample, there are four reduction peaks (near 2.76, 2.70, 2.49 and 2.11V) and three oxidation peaks (near 2.91, 2.84 and 2.45 V) between 1.8–3.0 V.

This should ascribes to main Li^+ ions intercalation and deintercalaton in different intermediate phases (tetrahedron site, two-phase coexist of LiV_3O_8 and $Li_4V_3O_8$, and $Li_4V_3O_8$ single phase) steps [7] and corresponds to the platforms in charge and discharge curves. In the region of 3.5–4.0 V there is

another reduction peak (near 3.61V) and oxidation peak (3.72 V), possible originating from the impurity phase in LiV_3O_8 sample. At the same time, the larger peaks areas of 350 ^oC–synthesized sample means to the higher discharge/charge capacities compared to the other samples synthesized at different temperatures. Besides this, it is found that redox potential difference (ΔE_p) of 350 ^oC–synthesized sample is smaller than that of 300 ^oC–synthesized one. It is well known that the less difference between the potential of the oxidation and reduction peaks, the better electrochemical reversibility. Therefore, 350 ^oC–synthesized sample displays the better electrochemical performance.

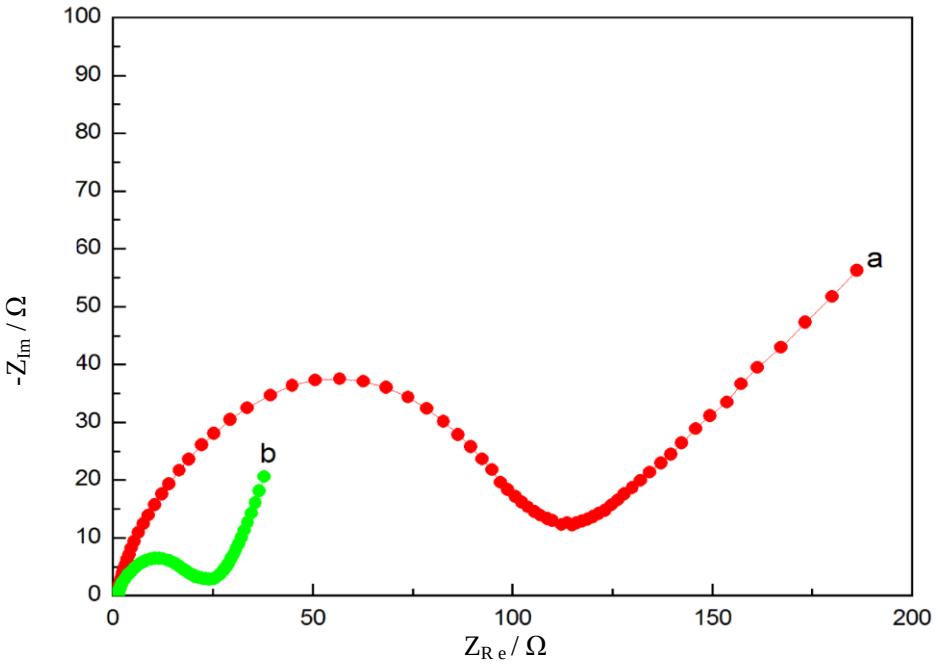

Figure 7. Electrochemical impedance spectra of 350 ^oC–synthesized sample at different states (a) open circuit voltage, (b) the fifth cycle at charge state

The Fig.7 presents the electrochemical impedance spectrum (EIS) of 350 ^oC–synthesized LiV_3O_8 sample. The Fig 7(a) shows EIS tested at open circuit voltage for the pristine state, and Fig 7(b) shows EIS at the charge state after five cycles. The spectra all consist of a semi-circle in the high frequency region and an inclined line at constant angle to the real axis at the low frequency. The semi-circle curve in the high frequency is attributable to the charge transfer (R_{ct}) between the electrode and electrolyte interface, while the line in the low frequency is due to the Li^+ ion diffusion in the solid electrode. The fitting R_{ct} for the two states are 113.4 Ω and 23.7 Ω, respectively. It is clearly that R_{ct} of the initial state is higher than that of the fifth cycle. This may be attributed to an active process of LiV_3O_8 material with cycling, which is favorable to Li^+ ion intercalation/deintercalaton and in accordance with the conclusion of H. Yang et al. [21].

4. CONCLUSIONS

In this work, we synthesize LiV_3O_8 powder by a new method which is based on binary Li-source wet chemistry system. XRD result implies that LiV_3O_8 phase can be formed at 250 ^oC and 300 ^oC–synthesized sample displays the highest crystallinity. SEM examination shows that 300 ^oC – synthesized sample has the largest partical size. From the electrochemical tests, we can see that the 350 ^oC–synthesized sample shows the higher initial specific capacity and better cycling stability, in contrast, the 300 ^oC–synthesized sample shows the poor electrochemical performance. EIS analysis manifests that 350 ^oC–synthesized sample may undergo an electrochemical active process in the first several cycles. Therefore, this facile wet chemistry synthesis route enriches the SCSMs concerning $Li_{1+x}V_3O_8$ synthesis and is worthy of further study.

ACKNOWLEDGEMENT

This work was sponsored by Program for Science & Technology Innovation Talents in Universities of Henan Province (HASTIT), China (Grant No. 2011HASTIT017), Young Core Teacher Program in Higher Education Institutions from the Education Commission of Henan Province, China (Grant No. 2009GGJS-059) and Zhengzhou Municipal Science & Technology Development Programs, China (Grant No. 112PZDZX019 and 2010GYXM641).

References

1. A.Yu, N. Kumagai, Z. Liu, J.Y. Lee, *J. Powder Sources* 74 (1998) 117.
2. H.Y. Xu, H. Wang, Z.Q. Song, Y.W. Wang, H. Yan, M. Yoshimura, *Electrochim. Acta* 49 (2004) 349.
3. H.W. Liu, H.M. Yang, T. Huang, *Mater. Sci. Eng*. B 143 (2007) 60.
4. V.R. Channu, R. Holze, E.H.W. Jr, S.A.W. Sr, R.R. Kalluru, Q.L.Williams, W. Walters, *Int. J. Electrochem. Sci*. 5 (2010) 1355.
5. Q.Y. Liu, H.W. Liu, X.W. Zhou, C.J. Cong, K.L. Zhang, *Solid State Ionics* 176 (2005) 1549.
6. X.Y. Cao, L.J. Guo, J.P. Liu, L.L. Xie, *Int. J. Electrochem. Sci*. 6 (2011) 270.
7. Y.C. Si, L.F. Jiao, H.T. Yuan, H.X. Li, Y.M. Wang, *J. Alloy Compd*. 486 (2009) 400.
8. Y.M. Liu, X.C. Zhou, Y.L. Guo, *Mater. Chem. Phys*. 114 (2009) 915.
9. L. Liu, L.F. Jiao, Y.H. Zhang, J.L. Sun, L. Yang, Y.L. Miao, H.T. Yuan, Y.M. Wang, *Mater. Chem. Phys.* 11 (2008) 565.
10. J.G. Xie, J.X. Li, H. Zhan, Y.H. Zhou, *Mater. Lett*. 57 (2003) 2682.
11. H.M. Liu, Y.G. Wang, W.S. Yang, H.S. Zhou, *Electrochim. Acta* 56 (2011) 1392.
12. H. Ma, Z.Q. Yuan, F.Y. Cheng, J. Liang, Z.L. Tao, J. Chen, *J. Alloy Compd*. 509 (2011) 6030.
13. Y. Zhou, H.F. Yue, X.Y. Zhang, X.Y. Deng, *Solid State Ionics* 179 (2008) 1763.
14. H.M. Liu, Y.G. Wang, K.X. Wang, Y.R. Wang, H.S. Zhou, *J. Power Sources* 192 (2009) 668.
15. A.Q. Pan, J.G. Zhang, G.Z. Cao, S.Q. Liang, C.M. Wang, Z.M. Nie, B.W. Arey, W. Xu, D.W. Liu, J. Xiao, G.S. Li, J. Liu, *J. Mater. Chem.* 21 (2011) 10077.
16. J.L. Sun, L.F. Jiao, X. Wei, W.X. Peng, L. Liu, H.T. Yuan, *J. Solid State Electrochem*. 14 (2010) 615.
17. F. Wu, L. Wang, C. Wu, Y. Bai, *Electrochim. Acta* 54 (2009) 4619.

18. Y.M. Liu, X.C. Zhou, Y.L. Guo, *J. Powder Sources* 184 (2008) 303.
19. S.H. Ju, Y.C. Kang, *Mater. Chem. Phys*. 126 (2011) 133.
20. J.Q. Xu, H.L. Zhang, T. Zhang, Q.Y. Pan, Y.H. Gui, *J. Alloy Compd.* 467 (2009) 327.
21. H. Yang, J. Li, X.G. Zhang, Y.L. Jin, *J. Mater. Process. Tech*. 207 (2008) 265.